52nd International Conference on Environmental Systems
16-20 July 2023, Calgary, Canada ICES-2023-77

Alternate Approach to Multi-Layer Insulation Modeling to Reduce Node Count

Hume L. Peabody[1] and Chris Evans[2]
NASA-GSFC, Greenbelt, MD 20771

For models with a limitation on the overall node count, the typical approach to Multi-Layer Insulation (MLI) modeling may generate nodes that are necessary for the analysis, but do not represent components of particular interest. This leaves fewer nodes that can be utilized to model components of greater importance than the MLI. A common approach to modeling MLI is to include a separate MLI node representing the outer layer of the insulation and a radiative coupling based on the area multiplied by an effective emissivity. Therefore, wherever insulation is included, one node is needed for the underlying surface and another node for the insulation. Since many spacecraft and instruments include MLI covering a sizable portion of their designs, this may result in a considerable number of nodes being used for MLI.

An alternate method to MLI modeling was developed that eliminates the MLI node, while still preserving the effect of the insulation for the underlying surface, thereby increasing the available nodes that could be used elsewhere in the model. This approach relies on preserving the baseline reflectivity, while reducing the absorptivity (based on the blanket effective emittance) and including a transparency. An inactive second surface is placed just behind the base surface that fully absorbs any energy that is transmitted without including its effect in the model. In essence, this approach applies only the energy that makes it through the blanket to the underlying surface. This method was tested out on the Roman Space Telescope model in local areas in preparation for its use in the generation of a launch model, which is constrained in the allowable node count. This paper documents the performance of the method and presents a comparison between the One-Node MLI method and the traditional two node MLI approach.

Nomenclature

α	= *Solar Absorptivity*
API	= *Application Programming Interface*
ε	= *Infrared Emissivity*
ε^*	= *Effective Emissivity*
F_{ij}/B_{ij}	= *View factor / Interchange Factor*
MLI	= *Multi-Layer Insulation*
ρ	= *Reflectivity*
RST	= *Roman Space Telescope*
τ	= *Transmissivity*

I. Introduction

Most thermal models of spacecraft include a substantial number of calculations points (or nodes) for modeling Multi-Layer Insulation (MLI), which is a very common thermal control component for spacecraft. Modeling of MLI has traditionally been handled in the same way for over five decades, with two nodes needed for each MLI location: one for the underlying surface temperature and a second for the outermost layer temperature. These two nodes are most often coupled together with a single radiative coupling whose value is based on the surface area and an effective emissivity (ε*), which is often derived from historical and empirical test data (typically in the range of 0.001 to 0.1).

For model deliveries with a constrained node count, this results in a significant number of nodes being needed to model all the various locations where MLI is utilized. A brief survey of recent and current missions at the Goddard Space Flight Center shows that around 25% of the total nodes were MLI. So, if a model delivery has a node limit of 10000 total nodes, only about 7500 nodes could be used for more important structure and component locations, with 2500 being needed just for modeling the MLI. Losing nearly a quarter of the available nodes could have a considerable impact on how the model gets built, with less fidelity available due to the lower node count available

[1] Staff Thermal Engineer, Mail Stop 545, Goddard Space Flight Center, Greenbelt MD 20771.
[2] Thermal Engineer, Mail Stop 545, Goddard Space Flight Center, Greenbelt MD 20771.

for more critical nodes. A method was sought to reduce the impact of MLI on node count to better utilize the available nodes for a launch model for the Roman Space Telescope (RST). The current flight RST model contains a total of 209,000+ nodes with 61,000+ being insulation nodes (about 29%). A reduced version of this model needs to be developed to deliver to the launch vehicle provider, for which a total node count of 10000 has been specified. There is a strong motivation to be able to better "spend" these nodes more wisely on portions of this model than to be forced to use them for MLI. While typical massless MLI node likely do not contribute significantly to run time, somewhat arbitrary node count limitations may not be negotiable based on contracts and organizations flexibility.

A method was proposed that utilizes a single node for each MLI instance but includes multiple surfaces with appropriate optical properties to properly reflect energy and absorb (and tally) only the energy that makes it *through* the insulation, while fully absorbing (but not tallying) the remaining energy. This method was tested on a smaller model to evaluate the approach. Once evaluated, the OpenTD Application Programming Interface (API) was utilized to automate the process to allow users to implement the method and update the model accordingly.

II. Background Derivation and Assumptions

MLI is often modeled with one node for the outer layer, one node for the underlying structure, and a single radiative coupling between them with a value based on the area (A) and an effective emissivity (ε*). The outer layer may have heat contributions, both incoming from and outgoing to, many other surfaces as well as incoming from sources (e.g. Planet Flux, Solar Flux, Albedo). Likewise, the inner layer may also have many radiative and conductive couplings to other nodes/surfaces as shown in Figure 1, Left. The goal of this effort was to try to find a way to remove the MLI node and adjust all the external couplings in a manner such that the total absorbed heat is equivalent to the heat transferred through the traditional Aε* coupling. If the correct net value of heat is transferred to or from the underlying surface node based on the adjusted external couplings, then the method could be used to eliminate the MLI node from the solution as shown in Figure 1, Right.

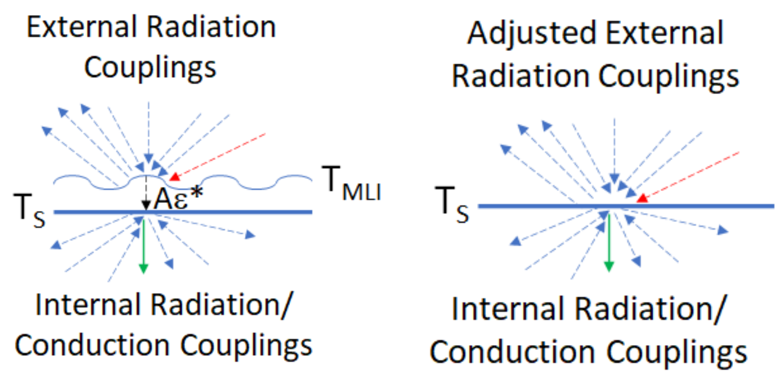

Figure 1. Typical Two-Node MLI Modeling: *Left shows a traditional method for modeling MLI with the directionally of heat inputs and outputs indicated. The Red arrow represents a solar load, which would be over a different wavelength spectrum and the green indicates a conductive path. Right shows a goal of similar connections, but whose values represent only the portion of the heat that gets to or leaves the underlying surface.*

It is relevant to identify that impressed heat loads from sources (e.g. Solar Flux) can alternately be represented by a coupling and interchange factor to a representative temperature of the source. In other words, impressed fluxes can be interchangeable with couplings between nodes (where one of the nodes represents a source/boundary). Furthermore, it should also be noted that an absorbed flux may be based on solar absorptivity from one source as indicated by the red arrows in Figure 1 (based on its energy wavelength distribution) or InfraRed emissivity, which is used in place of absorptivity over an InfraRed band of absorbed energy from another source. Once the load is absorbed, the wavelength band of the emitted energy may be different than that of the source,

Lastly, in this discussion, it is important to point out that MLI is designed to impede heat flow. As such, most of the absorbed external load is reradiated away. In general, the designs for most spacecraft seek to maximize the heat rejection of radiators, and as such, MLI is often designed to minimize emitted energy from the spacecraft through the MLI or reflected energy from external sources that could be absorbed by the radiators. Therefore, it is judged that a large part of the energy that is either reflected by or emitted from the MLI outer layer is most likely to reach deep space. Therefore, whether environmental loads come from an external source and are reflected back out to space or are absorbed and re-emitted back out to space, the end effect is that the majority of the associated external energy does not enter a control volume around the spacecraft that does not extend beyond the underlying MLI surfaces. To take this argument to the extreme conclusion, if all the insulation were perfect inhibitors of heat, then only reflected energy from external sources would impact the spacecraft as no internally generated heat could leave through the MLI. This does, however, point out the need of this approach to correctly model the reflective behavior from external sources.

Combining all the incoming and outgoing heat into a single load (akin to a test panel temperature to represent the effective thermal scene) allows a relatively gross simplification to be made as if the total load comes from one single individual source. Therefore, if the representation is from a single effective sink temperature (Figure 2), then the two serial radiative conductors can be represented as Area * (ε ε* / (ε + ε*)) between the sink temperature and the underlying surface temperature. This is acknowledged to be a fairly gross simplification, but in the absence of any additional parameters (such as temperature), during the radiative solution, options are quite limited. Extending this methodology to the surface properties allows for the emissivity to be degraded based on both the surface ε and the MLI ε*. The same approach is made for the α, although this is a bit harder to justify. Recall however that ε is used in place of absorptivity over a wavelength band related to emitted InfraRed energy and in the end only really applies to absorbed solar and albedo energy. Therefore, if the reflectivity remains the same, but the absorptivity/emissivity is degraded, this results in a non-zero transparency, which is addressed in the next section.

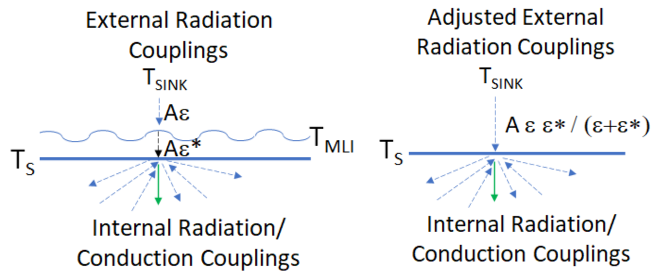

Figure 2. MLI Sink Temperature: *If the external radiative scene is represented by a single Equivalent Sink Temperature, then the two serial, radiative couplings can be combined into a single coupling and eliminate the intermediate MLI node*

III. The One-Node Insulation Method

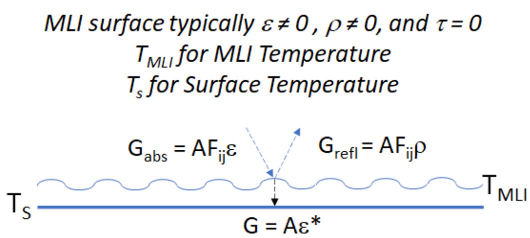

Figure 3. Typical Two-Node MLI Modeling: *MLI is often modeled using the outer layer properties for computed radiation and coupled to the underlying structure with a radiative conductor based on the area times an effective emissivity.*

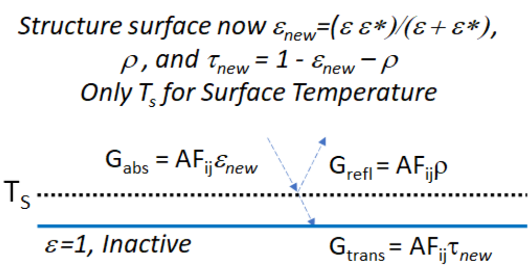

Figure 4. Proposed One-Node MLI Modeling: *This approach utilizes transparency and an inactive absorber to apply the energy making it through the blanket directly to the underlying surface*

The proposed method, hereafter termed the One-Node approach, attempts to preserve the reflectance behavior while adjusting the absorptance to a value based on the energy that gets through the insulation and is applied to the underlying surface; the remaining portion of energy is transmitted through and absorbed by a fully absorptive, but *radiatively inactive* surface. Recall from the discussion in Section II, that a majority of the external load is likely re-radiated to deep space; therefore, for a control volume around a spacecraft, but excluding the MLI, this energy never enters. Consequently, to first order, conservation of energy holds and the energy is not "lost" in the system. Figure 3 shows a typical schematic of how MLI is modeled on one side of a surface. Energy coming into the outer blanket layer is generally either reflected or absorbed. Of the energy that is absorbed, part of it may re-radiate away from the underlying structure and the remaining portion will go through the layers of the blanket and into the underlying structure. The mechanism by which heat gets through the blanket is more complex than simple conduction or radiation but is most often represented as a radiative coupling proportional to the surface area and an effective emissivity (ε*) whose value is often based on historical empirical or correlated data. Figure 4 shows the proposed One-Node MLI approach. In this configuration, the outer-most surface includes a degraded emissivity (ε ε*)/(ε + ε*), the same reflectivity, and a corresponding transmissivity to sum to unity. With a non-zero transmissivity, some energy will go through the surface, but a full absorber is placed just behind the surface and made inactive such that any absorbed energy is neglected. In essence the correct portion of energy is reflected by the reflectivity remaining the same and the absorbed energy includes only what makes it through the blanket, thereby removing the need to include a node for the outer layer.

IV. Implementation in Thermal Desktop

To configure a model for this new approach for a single sided surface (where the node numbers are the same on each side) with MLI on the "top/out" side, a second surface is created, very slightly offset (nominally 0.1 mm) from the base surface in the direction of the MLI with the same properties (node subdivision, material, thickness, etc) as the base surface. New optical properties are defined with both ε_{new} and α_{new} (where $\alpha_{new} = (\alpha\ \varepsilon^*) / (\alpha + \varepsilon^*)$, the same reflectivity (ρ) and a corresponding transmissivity (τ) to sum to unity. The new surface is then modified as follows: (1) MLI assignments are disabled, (2) the "top/out" side optical property is assigned the new property while (3) the "bottom/in" side is assigned as a perfect absorber ($\alpha = \varepsilon = 1$), (4) the activity is set such that the "top/out" side is active and the "bottom/in" side is inactive for radiation, and lastly (5) the thickness, material, node assignments and breakdown all remain as the base surface definitions, but the node/conductance generation is disabled. The base surface is also modified such that (1) the MLI assignment is disabled, (2) the "top/out" side is set to a perfect absorber and made inactive, (3) the "bottom/in" side retains its original optical properties and activity as long as it was unblanketed (the both sides blanketed case is discussed hereafter), and (4) the conductance and capacitance generation flag is left as is for the base surface. A schematic of this surface type before and after the updated configuration is shown in Figure 5. A similar effort is done for surfaces with MLI on both sides, but this approach requires additional transparent surfaces to be added to both sides of the base surface as shown in Figure 6.

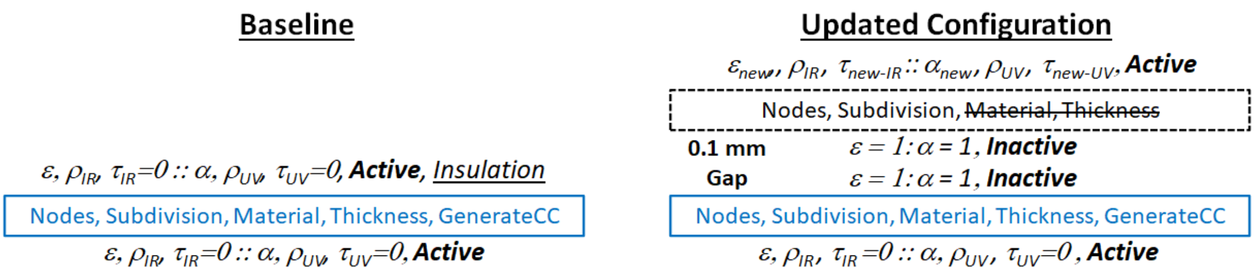

Figure 6. Model Modifications to Implement One-Node MLI Modeling (MLI on One Side): *This approach utilizes transparency and an inactive absorber to apply the energy making it through the blanket directly to the underlying surface*

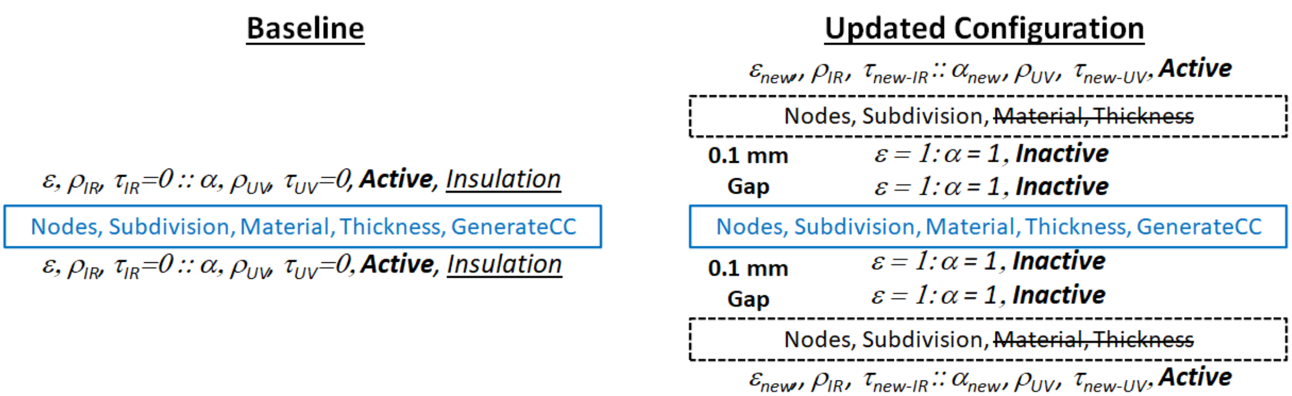

Figure 5. Model Modifications to Implement One-Node MLI Modeling (MLI on Both Sides): *This approach utilizes transparency and an inactive absorber to apply the energy making it through the blanket directly to the underlying surface on both sides of the base surface*

For these cases, it should be noted that the base surface is used for the generation of the conduction network and the spatial location of this surface in the Updated Configuration is identical to the Baseline so that merged nodes at adjoining surfaces do not become unmerged. Therefore, the conduction network generated is identical between the Baseline and the Updated Configuration. The only differences that may be found in the CondCap file generated by Thermal Desktop is the elimination of radiative coupling that is generated based on the inclusion of insulation.

The described approach is valid for planar surfaces but can easily be extended to revolved surface types (Cylinder, Cones, Paraboloids, etc) by adjusting radii (or possibly heights for closed types such as cones and paraboloids). Another potential concern is the application of this approach to quad elements that are non-planar. To address this, the offset direction is based on the average of the element normals for sub element 1-2-3 and 3-4-1 form quad element 1-2-3-4 as seen in Figure 7. As long as the angle between the two normals is not 180°, the resultant average vector direction should prevent the additional surfaces from intersecting the base surface, which could cause issues for the radiation ray tracing. While this was implemented in ThermalDesktop, the approach should also be able to be replicated in other thermal radiation codes that utilize Monte Carlo Ray Trace with a bit of effort.

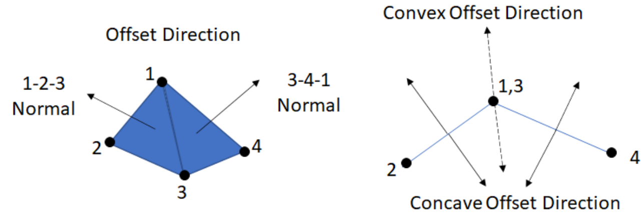

Figure 7. Accommodation of NonPlanar Quad Element: *For nonplanar, 4 sided elements, the 1-2-3 and 3-4-1 sub-element normals are averaged to determine the offset direction. The right image shows the same element with the view direction along the 13 vector*

V. Evaluation Model

A quick study was done on two localized regions of the RST observatory model, implementing the changes manually and the results looked promising. As such, a smaller, real-world model was selected (with less complexity and run time than the full RST) to further prove the concept. This model features many of the constructs with MLI that could prove problematic (non-planar quad elements, conic objects, partial MLI covering of single surface) and is shown in Figure 8.

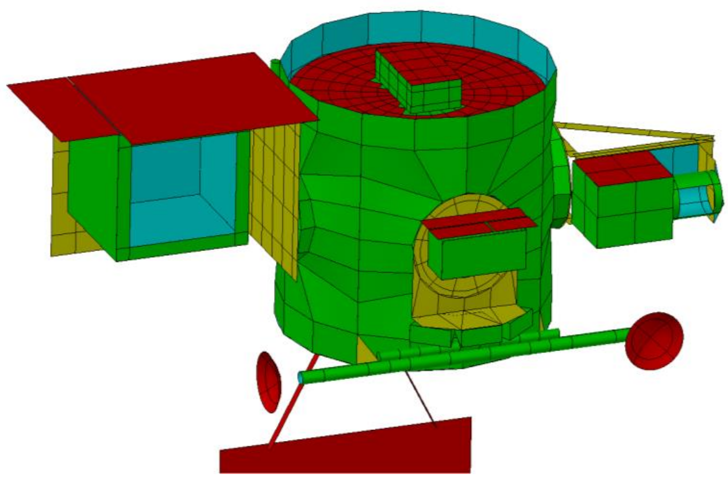

Figure 8. MLI on Evaluation Thermal Model: *Color coding for application of insulation: Green (MLI on visible side), Blue (MLI on non-visible side), Yellow (MLI on both sides), and Red (no MLI on either side)*

This model includes both quad and tri element shapes and as well as surfaces with MLI assigned to one or both sides. It also includes a number of primitive shapes with MLI (rectangles, disks, cylinders, etc.) Figure 8 shows the assembled view with indications of MLI color coded. Figure 9 highlights a transitional view showing the internals of the test case design. In essence, this model features three decks with dissipating components, with each deck coupled to the outer cylindrical structure. A fourth bottom deck serves as a closeout to solar intrusion for certain beta angles during the mission. The top-most deck has a dedicated, non-sun viewing direction throughout the mission and serves as the primary radiator. The model for the radiator also features partial MLI covering, utilizing the over-ride feature for both MLI assignment and optical properties. The 4 sets of

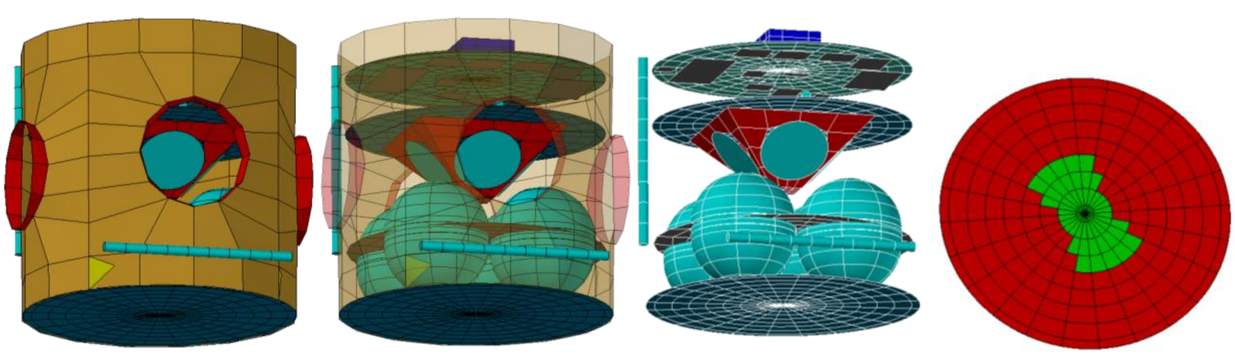

Figure 9. Transitional View of Evaluation Model: *The outer cylinder structure houses 4 internal decks; the top most serves as a radiator and the bottom most as a closeout. The top thee decks all support critical components*

instruments mounted to the ports are held as boundary temperatures and are not computed in the solution. This model served as the testbed to evaluate the technique once the code was developed to allow for easy implementation of the approach.

The code was developed in Visual Basic.NET using the OpenTDv63 API to access data for each surface in the model. If the surface included MLI, then it was further processed to establish the necessary optical properties. For planar primitive surface types (e.g. Rectangles, Disks, etc.), a copy is made of the surface and a translational offset is applied. For revolved surface types (e.g. Cone, Cylinder, etc), adjustments to radii and heights were made. For finite elements, a different approach was needed, as the shape of the element is defined by the nodes, rather than the node locations being defined by the surface. Therefore, the offset direction for top and bottom were determined based on the base element nodes and copies of these nodes are created, offset by the necessary distance and assigned as clone nodes. New elements are then created and the properties from the base element are copied to the new element. In all cases, the necessary optical properties, including the transparency were applied to the new surfaces, while the base surface was updated to be fully absorbing but inactive on the appropriate side. Conduction generation was disabled for all new surfaces, and MLI assignments removed from the base surface.

VI. Performance Predictions

Avg Temperature	**Baseline**	**One-Node**	***Avg Heater Power***	***Baseline***	***OneNode***
	(°C)	(°C)		*(W)*	*(W)*
Dissipation on Component A (66 W)	1.7	5.0	*Comp H Surv Heater*	*24.2*	*22.5*
Dissipation on Component B (13 W)	-2.8	-0.4	*Comp N2 - Mid*	*6.7*	*3.1*
Dissipation for Component C-1 (22 W)	12.7	19.0	*Comp N1 - Mid*	*7.2*	*3.2*
Dissipation for Component C-2 (22 W)	12.7	18.9	*Comp N3 - Mid*	*6.9*	*3.2*
Dissipation for Component C-3 (22 W)	12.8	19.0	*Comp N4 - Mid*	*6.6*	*3.2*
Dissipation for Component C-4 (22 W)	12.8	19.0	*Deck 1 Surv Heater B*	*32.1*	*20.1*
Dissipation of Comp_D (2 W / 3 Loc)	-0.3	3.8	*Deck 1 Surv Heater A*	*28.4*	*17.8*
Dissipation on Component E (1 W)	-3.4	-0.5	***Total***	***112.2***	***73.1***
Dissipation on Component F (8 W)	-1.0	1.9			
Dissipation on Component G (12 W)	-1.8	1.4			
Dissipation for Component H (46 W)	19.1	19.1			
Dissipation on Component I (34 W)	-2.4	-0.8			
Dissipation on Component J (9 W)	-1.0	1.6			
Dissipation on Component K (Varies)	1.8	2.6			
Dissipation on Component L (Varies)	1.2	3.3			
Dissipation on Component M (2 W)	-2.5	-0.4			

Figure 10. Temperature and Heater Comparison for Critical Components: *Critical component temperatures are shown for all dissipating components along with heater power demands for Component N and Deck 1*

The initial temperature predictions showed moderately good agreement (Figure 10), with some areas of the model clearly worse than others. Furthermore, the heater power predictions (also Figure 10) also showed some differences, with about 40 W less heater power needed for the One-Node MLI approach compared to the Baseline out of a total (Dissipation + Heater) power of 430 W. The dissipations were exactly equal between the two models as expected and totaled about 316 W. With heater control on Deck 1 and a large number of components mounted to this particular deck, the relatively close match of temperatures for components (excluding C, D, and H) is likely a direct result of the heater control and not necessarily related to the accuracy of the method. Figure 11 shows a histogram of the temperature error, with the One-Node approach generally predicting higher temperatures than the baseline MLI approach. Contour plots of the orbit average temperature differences are shown in Figure 12.

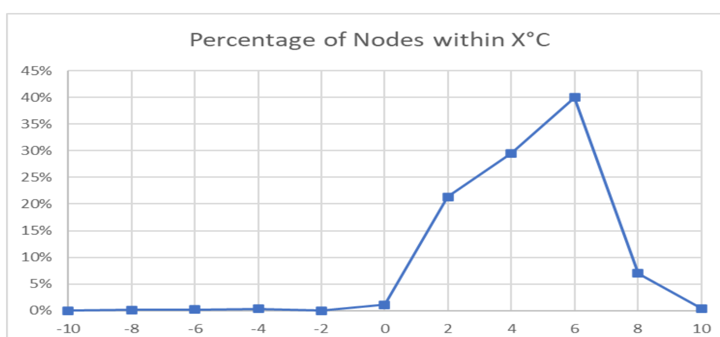

Figure 11. Histogram of Temperature Errors for all Mon-MLI Nodes: *Temperature Error (One-Node minus Baseline) is shown in buckets of 2 K, with the majority between 2 to 6°C error*

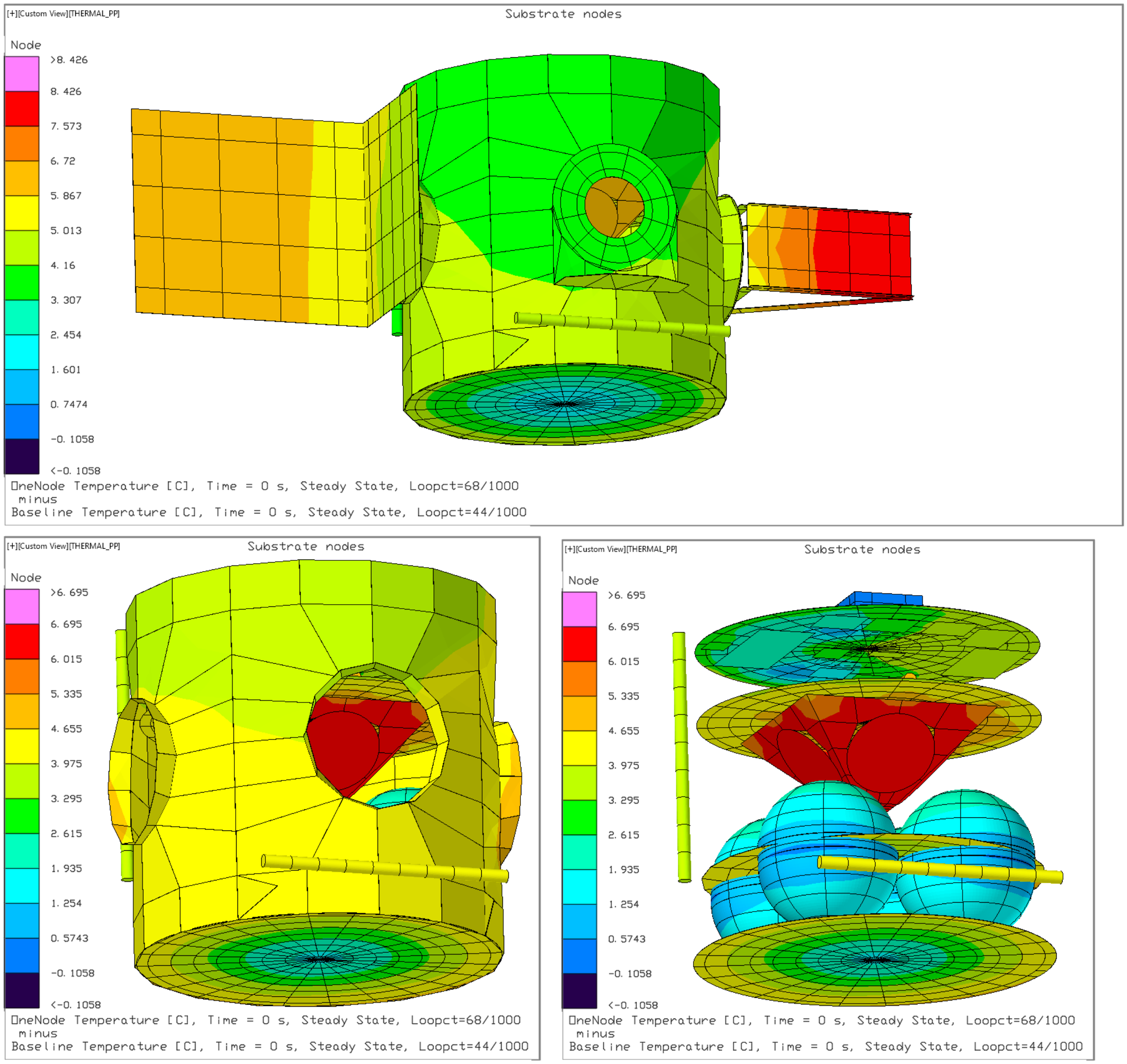

Figure 12. Contour Plot of Temperature Errors between Baseline and OneNode MLI Approaches: *The spatial distribution of temperature errors associated with the One-Node method are shown for the entire model (Top), main cylinder structure (Bottom Left) and internal components (Bottom Right)*

VII. Evaluation of Performance

With the agreement between the Baseline and the One-Node approach not as good as hoped, the heat flows in the evaluation model were further investigated. Overall, the heat flows, shown in Figure 13, do not appear to be significantly different, with the exception of areas where the absorbed environment differs greatly, which is mainly the structure. However, the large difference in the Structure environment is compensated by the larger heat rejected to space. To first order, the net heat flow exchange with the environment (Env – To Space) is quite similar, with the Baseline approach being 74.9 W and the One-Node approach being 69.2 W.

Other differences in dissipation are mainly driven by heater power differences as shown previously in Figure 10. For Deck 1, the difference is driven by the survival heaters A and B. For Deck 3, it is driven by the Component N heaters. The Deck Closeout initially appears to vary greatly, but in the baseline case, the heat that goes to the insulation is subsequently rejected to space, so in the end the Baseline case (1.5 + 18.9) is not significantly different

	Baseline	One-Node		Baseline	One-Node
Structure			**Deck 3**		
Environment	**47.1**	**137.8**	Environment	2.1	0.4
Dissipation	0	0	Dissipation	**30**	**18.8**
To Space	**122**	**207**	To Structure	28.3	18.2
To Insulation	0.1	0	To Space	2.5	0.7
To Deck 1	-10.1	4.2	To Insulation	1.3	0
To Deck 2	-57.7	-64.6	To Deck 2	-9.3	-2.7
To Deck 3	-28.3	-18.2	To Deck Closeout	6.4	3
To Deck Closeout	12.5	15.8			
Deck1			**Deck Closeout**		
Environment	59.2	58.7	Environment	0.4	0.4
Dissipation	**252.8**	**236**	Dissipation	0	0
To Structure	10.1	-4.2	To Structure	-12.5	-15.8
To Space	307	317.8	To Space	**1.5**	**27**
To Deck2	-11.6	-17.7	To Insulation	**18.9**	0
Deck2					
Environment	4	4			
Dissipation	88	88			
To Structure	57.6	64.6			
To Space	6.8	7			
To Deck 1	11.6	17.7			
To Deck 3	9.3	2.7			

Figure 13. Investigation of Heat Flows between Baseline and One-Node model: *The major heat paths from the Decks and the Structural Cylinder are shown to compare and contrast the model behavior for the two methods*

than the One-Node approach (27). In the end, it seemed to be mainly internal heat flow differences and directions of internal heat flows that caused the discrepancies seen in temperatures and heater powers.

Given the differences in the absorbed environmental heat flows, attempts were made to apply a universal scaling factor to the One-Node optical properties to allow for easy adjustment. A scale factor of greater than one results in an increase in the One-Node emissivity/absorptivity; the transmissivity is also subsequently adjusted to preserve the Baseline reflectivity which is derived from a summation to unity. The initial assumption was that a decreased emissivity/absorptivity was desirable to reduce the absorbed environmental flux, but this also had the unintended consequence of also reducing the radiation to space through the emissivity change. Analyses were also performed with a scale factor greater than one, but care had to be exercised that the scale factor did not produce a negative transmissivity, which is illegal. Overall, the application of a universal scale factor had a minimal effect on the performance.

At this point, the overall effectiveness of the method is considered inconclusive. It may be sufficient in some regions/cases of a model, while introducing unacceptable errors in other regions/cases. The sample problem was only evaluated for a single orbital cold case. Further cases at differing beta angles and under different hot and cold configurations is likely warranted before committing to either using the method or not. Furthermore, with the intent being for use in a launch model, the likelihood of needing considerable heater power is generally diminished, given the start of a transient launch analysis at room temperature and typically relatively low survival temperatures for components. A follow-up study could be considered which sets the heater power identical between the two methods to see the impact on temperature with consistent heatloads.

VIII. Implementation Lessons Learned

During the development of the code, a few obstacles were overcome that are worth sharing with the subset of the community who are interested in programming with the OpenTD API. When spawning a copy of an existing object, the framework includes a CopyProperties method under OpenTDv63.Utility.ObjectMapper. This method has numerous overloads to handle Rectangles, Disks, LinearQuads, etc. to allow one instance of an object to be cloned from another. However, care must be exercised when using this option as the handle is also copied. Since the handle is the unique identifier used by AutoCAD to exclusively reference each individual object, changes made to the copied object would also apply to the base object if the handles were the same. Furthermore, some of the properties that are copied are objects and not base data types. For these, it is actually the pointer being copied and not the value. Therefore, changes to these methods in the copied instance may also affect the base instance. To avoid these issues it is recommended to: 1) create a new object of the appropriate type and store the handle, 2) copy the base object to the target object using the CopyProperties method, 3) assign the handle from step 1 to the target object, 4) call the Update method to cast the target object back to Thermal Desktop, and finally 5) call the Get*ObjectType* method with the handle argument to retrieve a new instance of the target object, where *ObjectType* may be Rectangle, Disk, Cylinder, etc.. This approach establishes a "clean" instance of the object and avoids the pitfalls introduced by the CopyProperties method.

One other minor challenge to handle is the assertion if symbols or properties already exist. Since there is no method to see if a property exists, the easiest test is to use a Try…Catch approach. If the Try portion can access the symbol name, then the properties are updated; if the Try portion cannot access the symbol name, then the Catch portion allows for the creation and update of the symbol. A similar approach can be used with optical or thermophysical properties.

Lastly, when handling optical property changes to surfaces with over-ridden properties on insulation nodes, it is important to determine if the over-rides apply to the insulation nodes or the non-insulation nodes. For example, consider a surface with white paint, where nodes 1000-1004 have insulation applied with an MLI optical property; in this case the optical property over-rides to MLI should be applied to the corresponding insulation node numbers. However, it is also perfectly legal to assign the surface optical property to MLI and assign the overrides to all non-insulation nodes and assign them as white paint. If applying the One-Node MLI approach, it is important to identify which scheme is used, since the updates may be to the base surface property or the over-rides.

IX. Conclusions and Path Forward

The One-Node MLI approach did not provide as accurate a representation as the traditional two node approach but may be sufficiently accurate in localized areas. While no single issue was found to conclusively explain the differences, it is hypothesized that the complexity of radiative absorption and re-emission at the blanket outer layer coupled with the conduction and radiation through the blanket is more than can be simplified to a simple property change. In theory, it is hypothesized that there is a value for each blanket location that would produce the desired effect, but the determination of this value prior to solving for temperatures is likely impossible.

This approach will be further investigated on a localized area to see where or how it could be utilized to reduce node count while accepting the error introduced. The next steps in this effort will apply the technique only to the outer cylinder structure to see if external blankets that mainly view space and celestial sources more closely match between the two methods. A follow-on study is being considered to apply this technique only to internal blankets, which have far more complex views but generally no celestial loading. Furthermore, additional hot/cold and beta angle cases should be run to better evaluate the approach across multiple simulations.

Lastly, once the launch model is built for the RST project, the approach may be tried in selected areas to see if the node count can be reduced. The plan going forward is to build the model using the nominal two-node approach for MLI but allow the node count to exceed the threshold of 10000 nodes by the amount that removal of half of the MLI nodes would fit within the allocation. For example, if the model is 12000 nodes, of which 4000 are insulation, then assuming half of the nodes could be removed using this technique would yield 10000 nodes.

While the One-Node approach did not yield the accuracy initially desired, it also did not perform so poorly as to be ruled out for consideration. Clearly more data and test cases are needed with the hopes that trends and configurations can be identified that tip the scale either towards or away from its usage. For now, the approach should be employed at risk with the caveats that the performance may not be acceptable. As new evaluation and investigation of the technique becomes available it is hoped its recommendation (or not) for use will become clearer.

This work is presented to document what has been done so far in the event that others may wish to explore this approach more thoroughly. If resources permit, further investigations may be undertaken on less complex models. A realistic model with some complexity was initially sought to develop the code to implement the methodology, which is independent of the input model. Less complex models may be able to be utilized to further explore the limitations and weaknesses of the approach to either improve it or abandon its further use.

Acknowledgments

The primary author would like to thank the Roman Space Telescope project for continuing to support the exploration of analysis techniques and the OpenTD API to improve our processes.